International Journal of Automation and Computing 15(5), October 2018, 547-558
DOI: 10.1007/s11633-018-1145-8

Rotorcraft with a 3DOF Rigid Manipulator: Quaternion-based Modeling and Real-time Control Tolerant to Multi-body Couplings

J. Alvarez-Munoz[1] N. Marchand[2] J. F. Guerrero-Castellanos[3] J. J. Tellez-Guzman[2]
J. Escareno[4] M. Rakotondrabe[5]

[1] Polytechnic Institute of Advanced Sciences, FR 94200 Paris, France

[2] Univ. Grenoble Alpes, GIPSA-Lab, FR-38000 Grenoble, France

[3] Autonomous University of Puebla (BUAP), Faculty of Electronics, MX 72570 Puebla, Mexico

[4] University of Limoges ENSIL - ENSCI, XLIM Laboratory UMR CNRS 7252, Parc Ester Technopole, 16 rue Atlantis, Limoges 87068, France

[5] FEMTO-ST Institute, UMR CNRS-UFC/ENSMM/UTBM, Automatic Control and Micro-Mechatronic Department, FR Besançon, France

Abstract: This paper proposes a simple solution for the stabilization of a mini-quadcopter carrying a 3DoF (degrees of freedom) manipulator robot in order to enhance its achievable workspace and application profile. Since the motion of the arm induces torques which degrade the stability of the system, in the present work, we consider the stabilization of both subsystems: the quadcopter and the robotic arm. The mathematical model of the system is based on quaternions. Likewise, an attitude control law consisting of a bounded quaternion-based feedback stabilizes the quadcopter to a desired attitude while the arm is evolving. The next stage is the translational dynamics which is simplified for control (nonlinear) design purposes. The aforementioned controllers are based on saturation functions whose stability is explicitly proved in the Lyapunov sense. Finally, experimental results and a statistical study validate the proposed control strategy.

Keywords: Observer-based control, quaternion and Newton-Euler modeling, bounded-input control, aerial manipulator, disturbance rejection.

1 Introduction

Aerial manipulation has been an active area of research in recent times for unmanned aerial vehicles (UAVs) since it increases the application in both the military and civilian sectors. Unlike fixed-wing UAV configurations, whose flight profile lacks hovering flight, vertical take-off and landing (VTOL) rotorcrafts with three, four, six, or eight rotary propellers are well-suited for aerial manipulation operations. However, numerous scientific challenges, technological and theoretical, remain open. The main issue arises from their limited payload capacity. Thus, alternatively, multiple robots can carry heavier payloads using cables or grippers[1] which feature light and dexterous end-effectors. Furthermore, the dynamics of the robot is significantly altered while shifting and/or carrying payloads, due to the center of gravity shifting and external disturbances. Indeed, this is also an attraction in assembly because aerial robots can use this to sense disturbance forces and moments, as in [2]. Moreover, the performance of the aerial manipulation task relies on effective estimation of dynamic couplings for compensation purposes.

Numerous approaches have been proposed to deal with such problems. In [3], a Lyapunov based model reference adaptive control is used to stabilize a quadrotor with a multi degree of freedom (DoF) manipulator. However, the stability analysis is carried out with a linear approach and only the dynamics of the quadrotor was concerned due to the complexity of the system. Jimenez-Cano et al.[4] present a Newton-Euler approach to model and control a quadrotor through a variable parameter integral backstepping (VPIB) approach. However, the parametrization of the system is made through Euler angles, which present attitude estimation singularities. Kim et al.[5] present aerial manipulation using a quadrotor and a 2DoF robot arm. The dynamic model of the system is obtained by the Euler-Lagrange formulation. Then, an adaptive sliding mode controller is designed. The effective-

Research Article
Special Issue on Intelligent Control and Computing in Advanced Robotics
Manuscript received February 16, 2018; accepted June 29, 2018
Recommended by Guest Editor Jun-Zhi Yu

ness of the proposed method is showed experimentally by picking up and delivering an object.

In [6], the problem is solved through an autonomous avian-inspired grasping method, however the design of the controller is formulated in the vertical plane, which supposes a limitation to the full 3 D space. Sun et al.[7] present an amplitude-saturated nonlinear strategy for underactuated cranes with double-pendulum dynamics. Such a strategy is twice validated: theoretically and practically. The experimental platform consists of a car and a double-pendulum crane, where the coupling between the two systems (car and pendulum) is taken into account and a dynamic model is obtained. However, compared to an aerial vehicle, the attitude and position dynamics must be taken into account.

Finally, in [8], a new class of aerial manipulator is presented. It consists in a planar vertical take-off and landing (PVTOL) equipped with parallel manipulator arms attached to the center of mass (CoM) of the aerial vehicle, which is called protocentric. A control law has been proposed for the case of rigid joints and validated through simulations.

The contribution of the present paper is centered on a strategy that combines an alternative torque compensation approach with a nonlinear control design. Specifically, a mathematical model is presented in detail using quaternions and it takes into account the coupling between the two systems, quadcopter and manipulator. Unlike the research previously cited, the design of the attitude control law uses the quaternion parametrization, which avoids the presence of singularities.

With quaternion parametrization, we proposes a constructive control law for the attitude and position stabilization. First, the design of a smooth, almost globally asymptotical control law for attitude stabilization which takes into account the dynamics of the robotic arm, is carried out. After that, a globally asymptotical nonlinear controller for the translational dynamics is proposed. In general, the control law is based in the usage of a sum of nested saturation functions in order to take into account the actuator′s limitation. Real-time experimental results and a statistical study of the obtained results validate the proposed strategy.

The paper is structured as follows. In Section 2, the attitude model of the quadcopter with the manipulator arm is presented. Then, the attitude control design is formulated in Section 3. Section 4 gives a strategy to estimate the angular position of each link in the robot manipulator through a Luenberger observer. Section 5 is devoted to the design of the position control law. Section 6 presents the hardware setup, experimental results, as well as a statistical study. Finally, some conclusions are presented in Section 7.

2 System modeling

2.1 Unit quaternion and attitude kinematics

Consider two orthogonal right-handed coordinate frames: the body coordinate frame, $B(x_b, y_b, z_b)$, located at the center of mass of the rigid body and the inertial coordinate frame, $N(x_n, y_n, z_n)$, located at some point in the space (for instance, the earth north-east-down (NED) frame). The rotation of the body frame B with respect to the fixed frame N is represented by the attitude matrix $R \in SO(3) = \{R \in \mathbf{R}^{3\times 3} : R^{\mathrm{T}}R = I, \det R = 1\}$.

The cross product between two vectors $\xi, \varrho \in \mathbf{R}^3$ is represented by a matrix multiplication $[\xi^{\times}]\varrho = \xi \times \varrho$, where $[\xi^{\times}]$ is the well known skew-symmetric matrix.

The n-dimensional unit sphere embedded in $\mathbf{R}^{n+1}$ is denoted as $\mathbb{S}^n = \{x \in \mathbf{R}^{n+1} : x^{\mathrm{T}}x = 1\}$. Members of $SO(3)$ are often parameterized in terms of a rotation $\beta \in \mathbf{R}$ about a fixed axis $e_v \in \mathbb{S}^2$ by the map $\mathcal{U} : \mathbf{R} \times \mathbb{S}^2 \to SO(3)$ defined as

$$\mathcal{U}(\beta, e_v) = I_3 + \sin(\beta)[\mathrm{e}_v^{\times}] + (1 - \cos(\beta))[\mathrm{e}_v^{\times}]^2. \quad (1)$$

Hence, a unit quaternion, $q \in \mathbb{S}^3$, is defined as

$$q = \begin{pmatrix} \cos\dfrac{\beta}{2} \\ e_v \sin\dfrac{\beta}{2} \end{pmatrix} = \begin{pmatrix} q_0 \\ q_v \end{pmatrix} \in \mathbb{S}^3 \quad (2)$$

where $q_v = (q_1 \;\; q_2 \;\; q_3)^{\mathrm{T}} \in \mathbf{R}^3$ and $q_0 \in \mathbf{R}$ are known as the vector and scalar parts of the quaternion, respectively. The quaternion q represents an element of $SO(3)$ through the map $\mathcal{R} : \mathbb{S}^3 \to SO(3)$ defined as

$$\mathcal{R} := I_3 + 2q_0[q_v^{\times}] + 2[q_v^{\times}]^2. \quad (3)$$

Remark 1. $R = \mathcal{R}(q) = \mathcal{R}(-q)$ for each $q \in \mathbb{S}^3$, i.e., even quaternions q and $-q$ represent the same physical attitude.

Denoting by $\vec{\omega} = (\omega_1 \;\; \omega_2 \;\; \omega_3)^{\mathrm{T}}$ the angular velocity vector of the body coordinate frame B, relative to the inertial coordinate frame N, the kinematics equation is given by

$$\begin{pmatrix} \dot{q}_0 \\ \dot{q}_v \end{pmatrix} = \frac{1}{2}\begin{pmatrix} -q_v^{\mathrm{T}} \\ I_3 q_0 + [q_v^{\times}] \end{pmatrix}\vec{\omega} = \frac{1}{2}\Xi(q)\vec{\omega}. \quad (4)$$

The attitude error is used to quantify mismatch between two attitudes. If q defines the current attitude quaternion and q_d defines the desired quaternion, i.e., the desired orientation, then the error quaternion that represents the attitude error between the current orientation and the desired one is given by

$$q_e = q_d^{-1} \otimes q = (q_{e_0} \; q_{e_v}^{\mathrm{T}})^{\mathrm{T}} \tag{5}$$

where q^{-1} is the complementary rotation of the quaternion q which is given by $q^{-1} = (q_0 \quad -q_v^{\mathrm{T}})^{\mathrm{T}}$ and $\otimes$ denotes the quaternion multiplication[9].

2.2 Model of a quadcopter carrying a manipulator arm

The attitude dynamics and kinematics for the quadcopter have been reported in many works e.g., [10–12]. In these works the quadcopter mass distribution is considered to be symmetric. However, the mass distribution of a quadcopter with a manipulator is no longer symmetrical and varies with the movement of the arm. Consider a quadcopter with a manipulator arm with n links attached to its lower part. If the dynamics of the arm is neglected, the attitude kinematics and dynamics is given by

$$\begin{pmatrix} \dot{q}_0 \\ \dot{q}_v \end{pmatrix} = \frac{1}{2}\Xi(q)\vec{\omega} \tag{6}$$

$$J\dot{\vec{\omega}} = -\vec{\omega}^{\times} J\vec{\omega} + \Gamma_T \tag{7}$$

where $J \in \mathbf{R}^{3\times3}$ is the symmetric positive definite constant inertial matrix of the rigid body expressed in the body frame B and $\Gamma_T \in \mathbf{R}^3$ is the vector of applied torques. Γ_T depends on the (control) couples generated by the actuators, the aerodynamic couples such as gyroscopic couples, the gravity gradient or, as in the case of the present work, the couple generated by the movement of a robot manipulator placed under the body. Here, only the control couples, gyroscopic couples and the couple generated by the manipulator is considered in the control design. Consequently,

$$\Gamma_T = \Gamma + \Gamma_{arm} + \Gamma_G \tag{8}$$

where Γ and Γ_G will be described in Section 2.3. On the other hand, the vector Γ_{arm} is the torque generated by the total propulsive force being applied at the quadcopter geometric center which is displaced from the center of mass.

Taking the robot manipulator as a physical pendulum attached to the fuselage of the aerial vehicle and following a similar process to the one in [13], the manipulator torque can be computed by

$$\Gamma_{arm_{dyn}} = m_a g \zeta_{cd} \times \mathcal{R}(q) e_3 \tag{9}$$

where $\Gamma_{arm_{dyn}}$ is the manipulator torque taking into account the dynamics of each servomotor in the robot manipulator, $m_a = \Sigma_{i=1}^{n} m_{mi} + m_l$ is the total mass of the manipulator plus the load and $\zeta_{cd} = (\zeta_{c_x d} \; \zeta_{c_y d} \; \zeta_{c_z d})^{\mathrm{T}} \in \mathbf{R}^3$ is the position of center of mass of the quadrotor with respect to the pivot point. Then, the center of mass can be computed by

$$\zeta_{cd} = \frac{1}{m_a}\left[\sum_{i=1}^{n} m_{mi}\varrho_{id} + m_l \varrho_{ld}\right] \tag{10}$$

where ϱ_{id} and ϱ_{ld} are the position vectors of each link of the manipulator and the load, respectively, both with respect to the reference body frame given by the quadrotor.

In this case, let us consider the scheme in Fig. 1, which shows an anthropomorphic arm manipulator. This system has three degrees of freedom and then, the corresponding ϱ_{id}, where $i = \{1, 2, 3\}$, is given by

$$\begin{aligned}
\varrho_{1d} =& [0 \quad 0 \quad -l_{c1}]^{\mathrm{T}} \\
\varrho_{2d} =& [l_{c2}\sin\theta_{a2}\cos\theta_{a1} \quad l_{c2}\sin\theta_{a2}\sin\theta_{a1} \\
& -(l_1 + l_2)\cos\theta_{a2}]^{\mathrm{T}} \\
\varrho_{3d} =& [(l_2\sin\theta_{a2} + l_{c3}\sin(\theta_{a2}+\theta_{a3}))\cos\theta_{a1} \\
& (l_2\sin\theta_{a2} + l_{c3}\sin(\theta_{a2}+\theta_{a3}))\sin\theta_{a1} \\
& -(l_1 + l_2)\cos\theta_{a2} - l_{c3}\cos(\theta_{a2}+\theta_{a3})]^{\mathrm{T}}
\end{aligned} \tag{11}$$

where l_{c1}, l_{c2} and l_{c3} are the distances from the respective joint axes to the center of mass of each link, l_1, l_2 and l_3 are the total length of the links, and θ_{ai_m} measures the angular displacement from z and x axes. Then, since servomotors are used as actuators for the manipulator arm, these can be easily considered as first order systems. For this, a parameter identification is performed in order to know the different constant values of the motors. In general, the found system has the form:

$$\theta_{ai_m} = \frac{Ku(t) - \dot{\theta}_{ai_m}}{a} \tag{12}$$

where θ_{ai_m} is the angular position of the servo output shaft, $\dot{\theta}_{ai_m}$ is the angular velocity of the servo, a is a time constant linked to the time response of the servo, K is the gain of the system and $u(t)$ is the input.

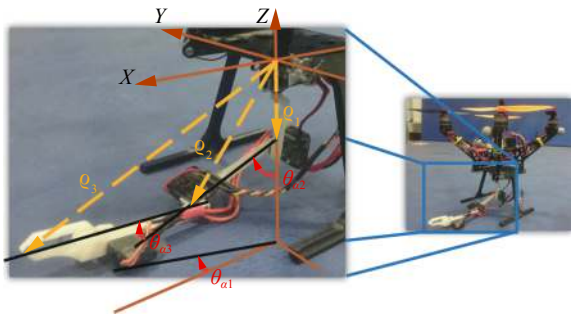

Fig. 1 Manipulator arm with three degrees of freedom

2.3 Actuator model

The quadrotor under study has four fixed-pitch rotors

mounted at the four ends of a simple cross frame. The model of the rotors is considered as a simple direct current (DC) motor which may reach high speed values (more than 200 rad/s). The collective input (or throttle input) is the sum of the thrusts of each rotor f_1, f_2, f_3, f_4. Therefore, the reactive couple Q_j generated in the free air by rotor j due to the motor drag and the total thrust T produced by the four rotors can be, respectively, approximated by

$$Q_j = ks_j^2 \tag{13}$$

$$T = \sum_{j=1}^{4} f_j = b\sum_{j=1}^{4} s_j^2 \tag{14}$$

where s_j represents the rotational speed of rotor j. $k > 0$ and $b > 0$ are two parameters which depend on the density of air, the radius, the shape, the pitch angle of the blade and other factors[12]. The vector of gyroscopic couples Γ_G is a consequence of the simultaneous rotation of the structure of the quadrotor and the high-speed rotation of the actuators, and it is given by

$$\Gamma_G = \sum_{j=1}^{4} J_r(\vec{\omega} \times \vec{z}_b)(-1)^{j+1} s_j \tag{15}$$

where J_r is the inertia of the so-called rotor (composed of the motor rotor itself with the gears). The components of the control torque $\Gamma \in \mathbf{R}^3$ generated by the rotors are given by $\Gamma = [\Gamma_1\ \Gamma_2\ \Gamma_3]^{\mathrm{T}}$, with

$$\Gamma_1 = d(f_3 - f_4) = db(s_3^2 - s_4^2) \tag{16}$$

$$\Gamma_2 = d(f_1 - f_2) = db(s_1^2 - s_2^2) \tag{17}$$

$$\Gamma_3 = -Q_1 - Q_2 + Q_3 + Q_4 = k(-s_1^2 - s_2^2 + s_3^2 + s_4^2) \tag{18}$$

where d is the distance between the rotor and the center of gravity of the quadrotor.

3 Attitude control design

3.1 Problem statement

The objective is to design a control law which drives the quadcopter to attitude stabilization under the torques and moments exerted to this from the movement of a manipulator arm attached to its lower part. In other words, let q_d denote the constant quadcopter stabilization orientation, then the control objective is described by the following asymptotic conditions

$$q \to [\pm 1\ 0\ 0\ 0]^{\mathrm{T}},\ \vec{\omega} \to 0 \text{ as } t \to \infty. \tag{19}$$

Furthermore, it is known that actuator saturation reduces the benefits of the feedback. When the controller continuously outputs infeasible control signals that saturate the actuators, system instability may follow. Then, besides the asymptotic stability, the control law also takes into account the physical constraints of the control system, in order to apply only feasible control signals to the actuators.

3.2 Attitude control with manipulator arm

In this subsection, a control law that stabilizes the system described by (6) and (7) is proposed. The goal is to design a control torque that is bounded.

Definition 1. Given a positive constant M, a continuous nondecreasing function $\sigma_M : \mathbf{R} \to \mathbf{R}$ is defined by

$$\sigma_M = s \quad \text{if } |s| < M$$
$$\sigma_M = \mathrm{sgn}(s)M \quad \text{elsewhere.} \tag{20}$$

Note that the components of Γ_{arm_i} are always bounded, i.e., $|\Gamma_{arm_i}| < \delta_i$. Then, one has the following result.

Theorem 1. Consider a rigid body rotational dynamics described by (6) and (7) with the following bounded control inputs $\Gamma = (\Gamma_1\ \Gamma_2\ \Gamma_3)^{\mathrm{T}}$ such that

$$\Gamma_i = -\sigma_{M_{i2}}\left(\Gamma_{arm_i} + \sigma_{M_{i1}}(\lambda_i[\omega_i + \rho_i q_i])\right) \tag{21}$$

with $i \in \{1, 2, 3\}$ and where $\sigma_{M_{i1}}$ and $\sigma_{M_{i2}}$ are saturation functions. Assuming $\delta_i < M_{i2} - M_{i1}$ and $M_{i1} \geq 3\lambda_i\rho_i$, where λ_i and ρ_i are positive parameters. Then the inputs (21) asymptotically stabilize the rigid body to the origin $(1\ 0^{\mathrm{T}}\ 0^{\mathrm{T}})^{\mathrm{T}}$(i.e.,$q_0 = 1$, $q_v = 0$ and $\vec{\omega} = 0$) with a domain of attraction equal to $\mathbb{S}^3 \times \mathbf{R}^3 \setminus (-1\ 0^{\mathrm{T}}\ 0^{\mathrm{T}})^{\mathrm{T}}$.

The proof of Theorem 1 is given in Appendix.

Remark 2. Note that the stability analysis has been carried out considering the asymptotic condition $q \to q_d = [\pm 1\ 0\ 0\ 0]^{\mathrm{T}}$. In th case where the asymptotic condition $q \to q_d$ with $q_d \neq [\pm 1\ 0\ 0\ 0]^{\mathrm{T}}$ is considered, the control law applied will be

$$\Gamma_i = -\sigma_{M_{i2}}\left(\Gamma_{arm_i} + \sigma_{M_{i1}}(\lambda_i[\omega_i + \rho_i q_{e_i}])\right) \tag{22}$$

where q_e represents the attitude error between the current orientation and the desired on.

4 Manipulator links angular position estimation

4.1 Problem statement

The objective is to design a strategy for the estimation of the angles on each link in the manipulator arm, combining the data coming from the first order model of the manipulator actuators and the data coming from the

end effector position tracked by the VICON system (motion capture system). Since the first order model does not fully describe the behavior of the arm manipulator (non-modeled dynamics, actuators malfunction, etc.). In order to know the angular positions of the manipulator links with respect to the base body (quadcopter), the inverse kinematics of the manipulator arm is used.

4.2 Manipulator links observer design

In this subsection, a Luenberger observer is designed to estimate the angles on each link in the manipulator. For this, the end-effector position is computed through the arm inverse kinematics to know the angle on each link. The expression that describes a link angle is given by

$$\theta_{aV} = \theta_a + \mu_V \tag{23}$$

where θ_{aV} is the estimated angle computed with the inverse kinematics, θ_a is the real angle and μ_V is a noise of minimal value. In addition, the observer allows the computation of the angular velocity. The expressions that represent the observer are given by

$$\dot{\hat{\theta}}_\delta = a\hat{\theta}_\delta + Ku_\delta + L(\theta_{aV} - \hat{\theta}) \tag{24}$$

$$\hat{\theta} = \hat{\theta}_V \tag{25}$$

where $\hat{\theta}_\delta$ is the estimated angle on a link in the manipulator, a and K are parameters of the first order system previously presented and L is a positive tuning parameter.

Now, given the expression (24), where $\hat{\theta}_\delta$ and $\dot{\hat{\theta}}_\delta$ were estimated, it is possible to compute the manipulator torque from (12) and use this new term as Γ_{arm} into the attitude control law (21).

5 Position control design

5.1 Problem statement

The objective is to design a control law which stabilizes the quadcopter to a desired position, thereby solving the attitude stabilization problem. In other words, once the control law has stabilized the attitude of the system, $\lim_{t\to\infty}(q, \vec{\omega}) = (q_d, \vec{0})$, the position control law should stabilize the quadcopter in a desired position, $\lim_{t\to\infty}(\vec{p}, \vec{v}) = (\vec{p}_d, \vec{0})$. This stabilization must be ensured even under the disturbances from the manipulator arm.

5.2 Position stabilization strategy

The schematic representation of a quadcopter carrying a manipulator arm can be seen in Fig. 2, where the inertial reference frame $N(x_n, y_n, z_n)$, the body reference

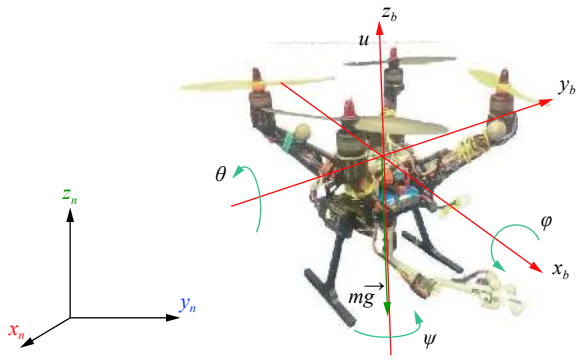

Fig. 2 Schematic configuration of a quadrotor carrying a manipulator arm

frame $B(x_b, y_b, z_b)$, the force u (thrust) and the weight vector $m\vec{g}$ are depicted. The dynamics of the whole system is obtained with the Newton-Euler formalism and the kinematics is represented using the quaternions formalism, given by

$$\Sigma_T : \begin{cases} \dot{\vec{p}} = \vec{v} \\ m_T\dot{\vec{v}} = -m_T\vec{g} + R\begin{pmatrix} 0 \\ 0 \\ u \end{pmatrix} \end{cases} \tag{26}$$

$$\Sigma_O : \begin{cases} \dot{q} = \frac{1}{2}\Xi(q)\vec{\omega} \\ J\dot{\vec{\omega}} = -\vec{\omega}^\times J\vec{\omega} + \Gamma_T \end{cases} \tag{27}$$

where $\vec{p}$ and $\vec{v}$ are linear position and velocity vectors, m_T is the total mass of the system (the quadcopter and the manipulator), $\vec{g}$ is the acceleration due to gravity, and R is the rotation matrix, given in (3).

Note that the rotation matrix R can also be given as a function of the Euler angles, i.e.,

$$R(\phi, \theta, \psi) = \begin{pmatrix} \mathrm{C}\psi\mathrm{C}\theta & \mathrm{S}\psi\mathrm{C}\theta & -\mathrm{S}\theta \\ \mathrm{C}\psi\mathrm{S}\theta\mathrm{S}\phi - \mathrm{S}\psi\mathrm{C}\theta & \mathrm{S}\phi\mathrm{S}\theta\mathrm{S}\psi + \mathrm{C}\psi\mathrm{C}\phi & \mathrm{C}\theta\mathrm{S}\phi \\ \mathrm{C}\psi\mathrm{C}\phi\mathrm{S}\theta + \mathrm{S}\psi\mathrm{S}\phi & \mathrm{S}\theta\mathrm{S}\psi\mathrm{C}\phi - \mathrm{C}\psi\mathrm{S}\phi & \mathrm{C}\theta\mathrm{C}\phi \end{pmatrix}. \tag{28}$$

Taking into account (26) and (27), this system can be seen as a cascade system, where the translational dynamics (26) depend on the attitude (27), but the attitude dynamics do not depend on the translational one. This property will be used to design the control law. Now, assume that using the control law (21) one can stabilize the yaw dynamics, i.e., $\psi = 0$, then after a sufficiently long time, system (26) becomes

$$\begin{pmatrix} \dot{p}_x \\ \dot{p}_y \\ \dot{p}_z \end{pmatrix} = \begin{pmatrix} v_x \\ v_y \\ v_z \end{pmatrix} \tag{29}$$

$$\begin{pmatrix}\dot{v}_x\\ \dot{v}_y\\ \dot{v}_z\end{pmatrix}=\begin{pmatrix}-\dfrac{u}{m_T}\sin\theta\\ \dfrac{u}{m_T}\sin\phi\cos\theta\\ \dfrac{u}{m_T}\cos\phi\cos\theta-g\end{pmatrix}. \tag{30}$$

With an appropriate choice of target configuration, it will be possible to transform (29) and (30) into three independent linear triple integrators. For this, take

$$\begin{aligned}\phi_d&=\arctan\left(\frac{r_2}{r_3+g}\right)\\ \theta_d&=\arcsin\left(\frac{-r_1}{\sqrt{r_1^2+r_2^2+(r_3+g)^2}}\right)\end{aligned} \tag{31}$$

where r_1, r_2 and r_3 will be defined after. Then, choose as positive thrust the input control

$$u=m_T\sqrt{r_1^2+r_2^2+(r_3+g)^2}. \tag{32}$$

Let the state be $p=(p_1,p_2,p_3,p_4,p_5,p_6,p_7,p_8,p_9)=(\int p_x,p_x,v_x,\int p_y,p_y,v_y,\int p_z,p_z,v_z)$, then (29) and (30) become

$$\Sigma_x:\begin{cases}\dot{p}_1=p_2\\ \dot{p}_2=p_3\\ \dot{p}_3=r_1\end{cases}\quad\Sigma_y:\begin{cases}\dot{p}_4=p_5\\ \dot{p}_5=p_6\\ \dot{p}_6=r_2\end{cases}\quad\Sigma_z:\begin{cases}\dot{p}_7=p_8\\ \dot{p}_8=p_9\\ \dot{p}_9=r_3.\end{cases} \tag{33}$$

Note that u will be always positive, and $u\geq mg$, in order to compensate the system's weight.

Since the chains of integrators given in (33) have the same form, a control law can be proposed as in [14], and can be established by Theorem 2.

Theorem 2. Consider the quadcopter translational dynamics expressed in (29) and (30). Then, the thrust input u given by (32) with r_1,r_2,r_3 as in (34), where $\sigma_{M_1}(\cdot)$ is defined in (20) with $M_1=1$ and ς_i are given by (35), $a_{(1,2,3)},b_{(1,2,3)},c_{(1,2,3)}>0$ tuning parameters such that $(a,b,c)_1>(a,b,c)_2+(a,b,c)_3$, $(a,b,c)_2>(a,b,c)_3$, stabilizes globally and asymptotically the quadcopter translational dynamics at the origin. Furthermore, if none of the σ_{M_1} are saturated, the poles of the linearized closed loop for the subsystems (33) reside at $-(a,b,c)_1$, $-(a,b,c)_2$, $-(a,b,c)_3$, respectively.

$$\begin{aligned}r_1=&-\varsigma_1\{a_3\sigma_{M1}[\frac{1}{\varsigma_1}(a_2p_1+p_2+p_3)]+\\ &a_2\sigma_{M1}[\frac{1}{\varsigma_1}(a_1p_2+p_3)]+a_1\sigma_{M1}[\frac{1}{\varsigma_1}(p_3)]\}\\ r_2=&-\varsigma_2\{b_3\sigma_{M1}[\frac{1}{\varsigma_1}(b_2p_4+p_5+p_6)]+\\ &b_2\sigma_{M1}[\frac{1}{\varsigma_2}(b_1p_5+p_6)]+b_1\sigma_{M1}[\frac{1}{\varsigma_2}(p_6)]\}\\ r_3=&-\varsigma_3\{c_3\sigma_{M1}[\frac{1}{\varsigma_1}(c_2p_7+p_8+p_9)]+\\ &c_2\sigma_{M1}[\frac{1}{\varsigma_3}(c_1p_8+p_9)]+c_1\sigma_{M1}[\frac{1}{\varsigma_3}(p_9)]\}\end{aligned} \tag{34}$$

$$\begin{aligned}\varsigma_1&=\frac{\bar{r}_1}{(a_1+a_2+a_3)}\\ \varsigma_2&=\frac{\bar{r}_2}{(b_1+b_2+b_3)}\\ \varsigma_3&=\frac{\bar{r}_3}{(c_1+c_2+c_3)}.\end{aligned} \tag{35}$$

Due to space constraints, the proof of Theorem 2 is not presented here, but it can be easily derived from the seminal work of [15–17] .

Remark 3. In the above Theorem 2, the stabilization goal is the origin. In the case where the asymptotic condition is different from the origin, the variables p_2,p_5,p_8 should be replaced in the control law (34) by $e_1=p_2-p_x^d$, $e_2=p_5-p_y^d$, $e_3=p_8-p_z^d$, respectively. In this case, p_x^d, p_y^d, p_z^d represent the desired position in the space.

6 Experimental validation

6.1 Hardware setup

In order to test the effectiveness of the proposed control law, a set of experiments were performed. The aerial system consists of a home-made quadcopter and arm manipulator, see Fig. 3. Both structures were specially designed and built for this project. The characteristics and parameters of each system are described in Table 1. The total weight of the quadcopter with its arm is 315 g and its carrying capacity is about 50 g.

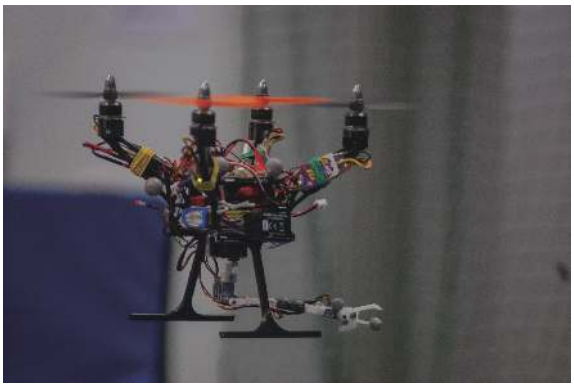

Fig. 3 Mini-quadcopter with its manipulator arm in flight

The attitude control law (21) for the quadcopter was programmed in a Microwii Copter board, which has gyros, accelerometers and the ATMega32u4 as processor. Then, a ground station estimates the position and attitude of the hexacopter using the Vicon Tracker system and T40s cameras[18]. With this system, it is possible to compute the position and attitude up to 100 Hz. The estimated states are sent to Matlab/Simulink through a user datagram protocol (UDP) frame every 2 ms. The position control algorithm is implemented in real-time at 200 Hz on a computer using number personal computer (xPC) target toolbox[19]. The control variables are finally

Table 1 Characteristics and parameters of the nano-hexacopter and the manipulator

System	Description	Value	Units
Quadcopter	Mass (m)	280	g
	Distance (d)	10.7	cm
	Battery	7.4	V
	Carrying capacity	80	g
	Inertial moment $x(J_\phi)$	0.0056	$kg \cdot m^2$
	Inertial moment $y(J_\theta)$	0.0056	$kg \cdot m^2$
	Inertial moment $z(J_\psi)$	0.0087	$kg \cdot m^2$
	Constant (b)	2615.23	N/s
	Constant (k)	257.80	N/s
Manipulator	Mass manipulator m_a	35	g
	Length 1st link l_1	5	cm
	Length 2nd link l_2	5	cm
	Length 3rd link l_3	8.4	cm

sent back to the quadcopter on the Microwii, through a Grenoble Image Parole Signal Automatique (GIPSA)-Lab's built-in bridge to DSM2 protocol. For this, a radio-frequency emitter is used. Furthermore, the manipulator arm is controlled by the DS35 Digital Super Sub-Micro Servo[20]. To transmit the control signals to the manipulator, Spektrum digital spread modulation 2 (DSM2) transmitters are connected to the ground station through another built-in bridge. An overview of the whole hardware architecture is presented in Fig. 4.

6.2 Experimental scenario

A set of experiments is carried out in order to compare the performance of the proposed control with and without accounting for the torque generated by the manipulator, scenarios 1 and 2, respectively. The parameters of the control laws are selected according to the characteristics of the quadrotor actuators and the condition for the manipulator arm. For the attitude control law (21) and the position control law given in (34), where $\max|\Gamma_{armi}| = 0.085\,8\,\text{Nm}$ and $\delta_i = 0.1$, the next parameters values are proposed: $M_{11,21,31} = 0.1$, $M_{12,22,32} = 0.5$, $\lambda_{1,2} = 0.015$, $\lambda_3 = 0.013$, $\rho_{1,2} = 10.5$ and $\rho_3 = 11$. For the control (34), $a_1 = b_1 = 2.3$, $c_1 = 1.65$, $a_2 = b_2 = 1.2$, $c_2 = 0.55$, $a_3 = b_3 = 0.1$, $c_3 = 0.015$ and $\bar{r}_{1,2,3} = 5$. The experiments consist in two parts. First, the links of the manipulator arm are initialized to $\theta_{ai} = (0°\ 90°\ 0°)^{\mathrm{T}}$ and the quadrotor is driven to the position $\vec{p}_d = (0\ 0\ 1)^{\mathrm{T}}$. At time 20 s, $\theta_{ai} = (40°\ 30°\ 0°)^{\mathrm{T}}$. At time 25 s, $\theta_{ai} = (-30°\ 70°\ 25°)^{\mathrm{T}}$. At time 30 s, $\theta_{ai} = (10°\ 20°\ 35°)^{\mathrm{T}}$. Finally, at time 35 s, $\theta_{ai} = (0°\ 90°\ 60°)^{\mathrm{T}}$ and the quadrotor lands.

6.3 Experimental results in scenario 1

Fig. 5 shows the general performance of the aerial system under the disturbances coming from the manipulator arm when the arm torque estimation is not taken into account. Fig. 5 shows the angular and linear positions of the quadcopter during the experiment. Note that even when the quaternion parametrization is considered, Euler angles given in (28) are used in order to have a better perspective of the behavior of the system. In this case, attitude stabilization is guaranteed, but the movement of the manipulator causes stability issues for both attitude and linear position.

6.4 Experimental results in scenario 2

Fig. 6 shows the angular and linear positions of the quadrotor as well as the computed manipulator torques. The arm perturbations are compensated through the dynamic model and it results in a general stabilization improvement of the quadrotor compared to the precedent approach. In addition, the importance of this approach is that the precision of the angular position knowledge is enhanced, which guarantees a better torque estimation.

6.5 Results analysis and statistical study

In order to compare the obtained results of the proposed methods and the flight performance of the aerial vehicle under the disturbances coming from the movement of the manipulator arm, a statistical error study is

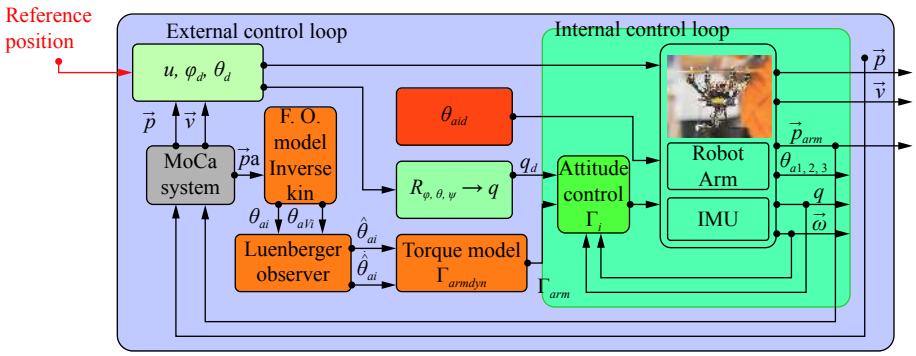

Fig. 4 Block diagram of the system

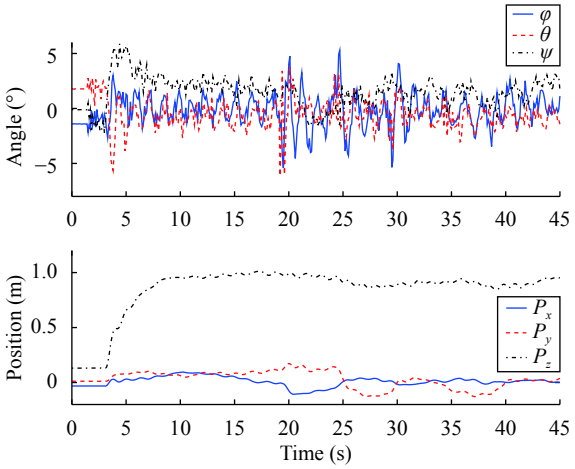

Fig. 5 General behavior of the system during scenario 1

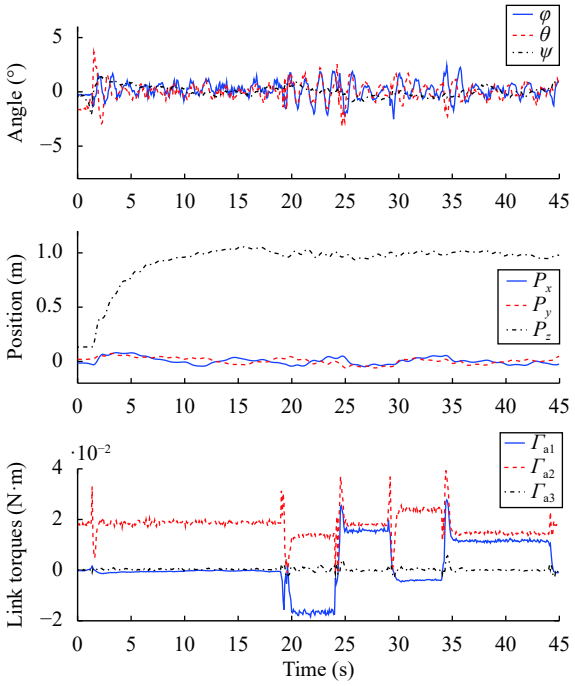

Fig. 6 General behaviour of the system during the experiment using dynamic method estimation torque compensation and the nonlinear observer

carried out. For this, the experiments described before were performed 8 times.

Figs. 7–9 show the linear position errors, the normal Gaussian distribution errors and the attitude errors for scenarios 1 and 2, respectively.

In order to calculate the attitude error, $\|2\arccos q_0\|$ was used, where $\|\cdot\|$ represents the norm and q_0 was defined as before. The obtained results show that the average attitude error when the dynamic method estimation is applied is reduced, compared with that obtained when the classical approach is implemented.

Since the attitude stabilization of the aerial robot is enhanced with the usage of the proposed method, then the linear position stabilization is equally improved, as it

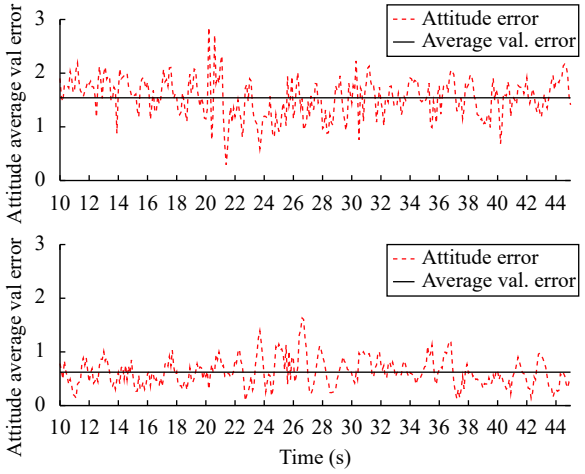

Fig. 7 Attitude error and attitude average error value during the different experiments

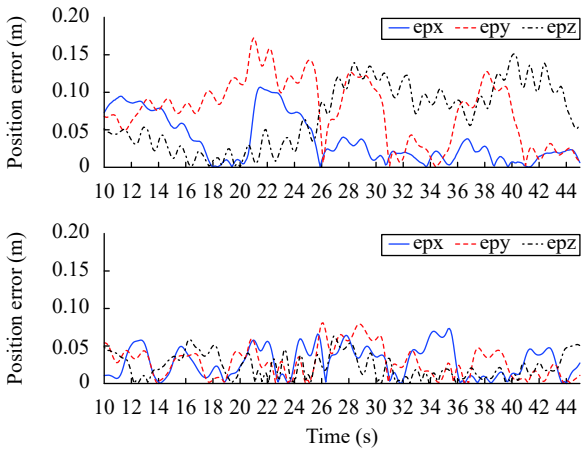

Fig. 8 Position errors during the different experiments

is shown in the linear position errors computation.

To have another perspective of the obtained results, the normal Gaussian distribution errors are computed. For this, the linear position errors data were used. Then, from the obtained distributions, it is clear that when the dynamic method estimation for the arm manipulator torque is used, the average error value is closer to 0. Furthermore, the area covered by the distributions when the classical approach is used is bigger, consequently, the probability of error increases.

In general, the stabilization of the system is improved and guaranteed with the use of the dynamic model and the nonlinear observer. Table 2 shows the different average error values for the set of experiments. The first column shows the attitude average value error, the second, third and fourth columns show the average error value for the x-axis, y-axis and z-axis. Since the experiment was repeated 8 times using the different approaches, Table 2 gives a better perspective of the stabilization improvement for both quadrotor attitude and linear positions, showing the effectiviness of the proposed approach.

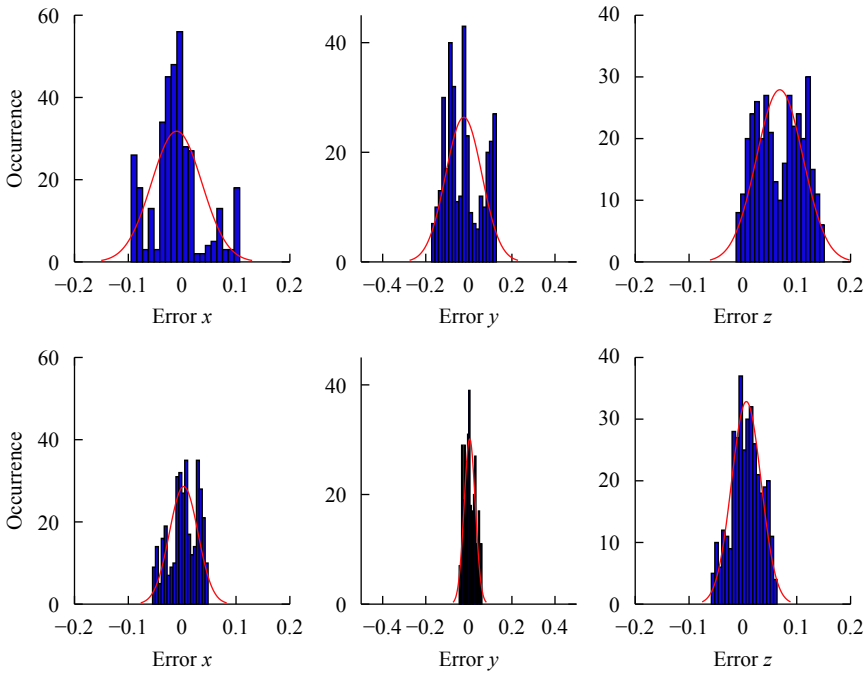

Fig. 9 Error Gaussian normal distributions

Table 2 Average error values for the experiment

Average error value	Orientation	Pos x	Pos y	Pos z
Scenario 1	1.5312	0.0375	0.0777	0.0468
	1.5411	0.0361	0.0762	0.0690
	1.4901	0.0341	0.0681	0.0335
	1.4320	0.0683	0.0728	0.0552
	1.3941	0.0525	0.0679	0.0592
	1.4480	0.0507	0.0538	0.0347
	1.4175	0.0489	0.0674	0.0404
	1.4520	0.0542	0.0702	0.0532
Total average error	1.4632	0.0477	0.0692	0.049
Scenario 2	0.6223	0.0294	0.0283	0.0230
	0.6034	0.0231	0.0344	0.0239
	0.6197	0.0251	0.0323	0.0278
	0.5714	0.0214	0.0234	0.0229
	0.6524	0.0269	0.0289	0.0189
	0.6277	0.0247	0.0277	0.0245
	0.5998	0.0225	0.0239	0.0239
	0.6308	0.0279	0.0302	0.0246
Total average error	0.6159	0.0251	0.0286	0.0236

7 Conclusions

In this paper, a novel model for a quadcopter carrying a manipulator arm was proposed. In addition, a control law was designed to asymptotically stabilize the attitude and position of the system. Moreover, this work has presented a method for aiding the solution through the design of a feed-forward term which allows the estimation of the moments and torques exerted by the manipulator. Since input constraints exist in the actuators, the control law takes into account the actuator's saturations. Experimental results and a statistical study show the effectiveness of the proposed control law in facing the disturbances coming from the manipulator. In a future work, experimental mass estimation and outdoor picking up and delivery of an object will be pursued.

Appendix

Proof of Theorem 1

Consider the candidate Lyapunov function V, which is positive definite.

$$V = \frac{1}{2}\vec{\omega}^{\mathrm{T}} J \vec{w} + \kappa((1-q_0)^2 + q_v^{\mathrm{T}} q_v) = \frac{1}{2}\vec{\omega}^{\mathrm{T}} J \vec{w} + 2\kappa(1-q_0) \tag{36}$$

where J is defined as before, and $\kappa > 0$ must be determined. The derivative of (36) after using (6) and (7) is given by

$$\begin{aligned} \dot{V} = {} & \vec{\omega}^{\mathrm{T}} J \dot{\vec{\omega}} - 2\kappa \dot{q}_0 = \\ & \vec{\omega}^{\mathrm{T}}(-\vec{\omega}^{\times} J\vec{\omega} + \Gamma + \Gamma_{arm} + \Gamma_G) + \kappa q_v^{\mathrm{T}} \vec{\omega} = \\ & \underbrace{w_1(\Gamma_1 + \Gamma_{arm_1}) + \kappa q_1 \omega_1}_{\dot{V}_1} + \\ & \underbrace{w_2(\Gamma_2 + \Gamma_{arm_2}) + \kappa q_2 \omega_2}_{\dot{V}_2} + \\ & \underbrace{w_3(\Gamma_3 + \Gamma_{arm_3}) + \kappa q_3 \omega_3}_{\dot{V}_3} \end{aligned} \tag{37}$$

where $\dot{V}$ is the sum of the three terms $(\dot{V}_1, \dot{V}_2, \dot{V}_3)$. First,

$\dot{V}_1$ is analyzed. From Γ_1 in (21) and (37), one gets

$$\dot{V}_1 = \omega_1(-\sigma_{M_{12}}(\Gamma_{arm_1} + \sigma_{M_{11}}(\lambda_1[\omega_1 + \rho_1 q_1])) + \Gamma_{arm_1}) + \kappa q_1 \omega_1 \quad (38)$$

if we choose $\delta_1 < M_{12} - M_{11}$, $\sigma_{M_{12}}$ is always operating in its linear region so $\dot{V}_1$ becomes

$$\dot{V}_1 = -\omega_1 \sigma_{M_{11}}(\lambda_1[\omega_1 + \rho_1 q_1]) + \kappa q_1 \omega_1. \quad (39)$$

Assume that $|\omega_1| > 2\rho_1$, i.e., $\omega_1 \in [2\rho_1, +\infty]$. Since $|q_1| \leq 1$, it follows that $|\omega_1 + \rho_1 q_1| \geq \rho_1 + \epsilon$ for any $\epsilon > 0$ sufficiently small. Therefore, $\omega_1 + \rho_1 q_1$ has the same sign as ω_1. From (39) and the norm condition on the quaternion, $\dot{V}_1$ takes the following form:

$$\dot{V}_1 = -\omega_1 \sigma_{M_{11}}(\lambda_1[\omega_1 + \rho_1 q_1]) + \kappa \omega_1 q_1 \leq -|\omega_1| \sigma_{M_{11}}(\lambda_1(\rho_1 + \epsilon)) + \kappa|\omega_1|. \quad (40)$$

Taking

$$\kappa < \min(M_{11}, \lambda_1 \rho_1 + \epsilon) \quad (41)$$

one can assure the decrease of V_1, i.e., $\dot{V}_1 < 0$. Consequently, ω_1 enters $\Phi_1 = \{\omega_1 : |\omega_1| \leq 2\rho_1\}$ in finite time t_1 and remains in it thereafter. In this case, $(\omega_1 + \rho_1 q_1) \in [-3\rho_1, 3\rho_1]$.

Let M_{11} verify the next inequality $M_{11} \geq 3\lambda_1 \rho_1$, (41) then becomes

$$\kappa < \lambda_1 \rho_1 + \epsilon. \quad (42)$$

For $t_2 > t_1$, the argument of $\sigma_{M_{11}}$ will be bounded as follows:

$$|\lambda_1(\omega_1 + \rho_1 q_1)| \leq 3\lambda_1 \rho_1 \leq M_{11}. \quad (43)$$

Consequently, σ_{M1} operates in a linear region:

$$\Gamma_1 = -\lambda_1[\omega_1 + \rho_1 q_1]. \quad (44)$$

As a result, (39) becomes

$$\dot{V}_1 = -\lambda_1 \omega_1^2 - \lambda_1 \rho_1 \omega_1 q_1 + \kappa \omega_1 q_1. \quad (45)$$

Choosing $\kappa = \lambda_1 \rho_1$ which satisfies inequality (42), one obtains:

$$\dot{V}_1 = -\lambda_1 \omega_1^2 \leq 0. \quad (46)$$

The same argument is applied to $\dot{V}_2$ and $\dot{V}_3$, (37) becomes

$$\dot{V} = \dot{V}_1 + \dot{V}_2 + \dot{V}_3 = -(\lambda_1 \omega_1^2 + \lambda_2 \omega_2^2 + \lambda_3 \omega_3^2) \leq 0. \quad (47)$$

In order to complete the proof, the LaSalle invariance principle is invoked. All the trajectories converge to the largest invariant set $\bar{\Omega}$ in $\Omega = \{(q_v, \vec{\omega}) : \dot{V} = 0\} = \{(q_v, \vec{\omega}) : \vec{\omega} = 0\}$. In the invariant set, $J\dot{\vec{\omega}} = -[\lambda_1 \rho_1 q_1 \ \lambda_2 \rho_2 q_2 \ \lambda_3 \rho_3 q_3]^{\mathrm{T}} = 0$, i.e., $\bar{\Omega}$ is reduced to the origin. This ends the proof of the asymptotic stability of the closed loop system. □

Acknowledgements

This work was supported by CONACYT-Mexico, LabEx PERSYVAL-Lab (No. ANR-11-LABX-0025) and Equipex ROBOTEX (No. ANR-10-EQPX-44-01).

References

[1] D. Mellinger, M. Shomin, N. Michael, V. Kumar. Cooperative grasping and transport using multiple quadrotors. In *Proceedings of International Symposium on Distributed Autonomous Robotic Systems*, Springer, Lausanne, Switzerland, pp. 545–558, 2010.

[2] M. Mohammadi, A. Franchi, D. Barcelli, D. Prattichizzo. Cooperative aerial tele-manipulation with haptic feedback. In *Proceedings of IEEE/RSJ International Conference on Intelligent Robots and Systems*, Daejeon, South Korea, pp. 5092–5098, 2016. DOI: 10.1109/IROS.2016.7759747.

[3] M. Orsag, C. Korpela, S. Bogdan, P. Oh. Lyapunov based model reference adaptive control for aerial manipulation. In *Proceedings of International Conference on Unmanned Aircraft Systems*, IEEE, Atlanta, USA, pp. 966–973, 2013. DOI: 10.1109/ICUAS.2013.6564783.

[4] A. E. Jimenez-Cano, J. Martin, G. Heredia, A. Ollero, R. Cano. Control of an aerial robot with multi-link arm for assembly tasks. In *Proceedings of IEEE International Conference on Robotics and Automation*, Karlsruhe, Germany, pp. 4916–4921, 2013. DOI: 10.1109/ICRA.2013.6631279.

[5] S. Kim, S. Choi, H. J. Kim. Aerial manipulation using a quadrotor with a two DOF robotic arm. In *Proceedings of IEEE/RSJ International Conference on Intelligent Robots and Systems*, Tokyo, Japan, pp. 4990–4995, 2013. DOI: 10.1109/IROS.2013.6697077.

[6] J. Thomas, G. Loianno, J. Polin, K. Sreenath, V. Kumar. Toward autonomous avian-inspired grasping for micro aerial vehicles. *Bioinspiration and Biomimetics*, vol. 9, no. 2, Article number 025010, 2014. DOI: 10.1088/1748-3182/9/2/025010.

[7] N. Sun, Y. C. Fang, H. Chen, B. Lu. Amplitude-saturated nonlinear output feedback antiswing control for underactuated cranes with double-pendulum cargo dynamics. *IEEE Transactions on Industrial Electronics*, vol. 64, no. 3, pp. 2135–2146, 2017. DOI: 10.1109/TIE.2016.2623258.

[8] B. Yuksel, G. Buondonno, A. Franchi. Differential flatness and control of protocentric aerial manipulators with any number of arms and mixed rigid-/elastic-joints. In *Proceedings of IEEE/RSJ International Conference on Intelligent Robots and Systems*, Daejeon, South Korea, pp. 561–566, 2016. DOI: 10.1109/IROS.2016.7759109.

[9] M. D. Shuster. A survey of attitude representations. *The Journal of the Astronautical Sciences*, vol. 41, no. 4, pp. 439–517, 1993.

[10] P. Castillo, A. Dzul, R. Lozano. Real-time stabilization and tracking of a four-rotor mini rotorcraft. *IEEE Transactions on Control Systems Technology*, vol. 12, no. 4, pp. 510–516, 2004. DOI: 10.1109/TCST.2004.825052.

[11] J. F. Guerrero-Castellanos, N. Marchand, N. Hably, S. Lesecq, J. Delamare. Bounded attitude control of rigid bodies: Real-time experimentation to a quadrotor mini-helicopter. *Control Engineering Practice*, vol. 19, no. 8, pp. 790–797, 2011. DOI: 10.1016/j.conengprac.2011.04.004.

[12] A. Alaimo, V. Artale, C. Milazzo, A. Ricciardello, L. Trefiletti. Mathematical modeling and control of a hexacopter. In *Proceedings of International Conference on Unmanned Aircraft Systems*, IEEE, Atlanta, USA, pp. 1043–1050, 2013. DOI: 10.1109/ICUAS.2013.6564793.

[13] S. Cho. Dynamics and Control of Underactuated Multibody Spacecraft, Ph. D. dissertation, University of Michigan, USA, 2002.

[14] R. Cruz-Jose, J. F. Guerrero-Castellanos, W. F. Guerrero-Sánchez, J. J. Oliveros-Oliveros. Global stabilizarion of a VTOL mini aircraft. In *rocedings of the National Conference of Automatic Control*, Campeche, Mexico, pp. 180–185, 2012.

[15] N. Marchand, A. Hably. Global stabilization of multiple integrators with bounded controls. *Automatica*, vol. 41, no. 12, pp. 2147–2152, 2005. DOI: 10.1016/j.automatica.2005.07.004.

[16] A. R. Teel. Global stabilization and restricted tracking for multiple integrators with bounded controls. *Systems & Control Letters*, vol. 18, no. 3, pp. 165–171, 1992. DOI: 10.1016/0167-6911(92)90001-9.

[17] E. N. Johnson, S. K. Kannan. Nested saturation with guaranteed real poles. In *Proceedings of American Control Conference*, IEEE, Denver, USA, vol. 1, pp. 497–502, 2003. DOI: 10.1109/ACC.2003.1239062.

[18] VICON, [Online], Available: http://www.vicon.com/products/camera-systems.

[19] Build, run, and test real-time applications, [Online], Available: http://fr.mathworks.com/products/simulink-real-time/, December 2017.

[20] E-flite RC, [Online], Available: http://www.horizonhobby.com/content/e-flite-rc.

J. Alvarez-Munoz received the M. Sc. degree in electronics from the Autonomous University of Puebla, Mexico in 2012, and the Ph. D. degree in automatic control from GIPSA-Lab, University of Grenoble (UGA), France in 2017. Currently, he holds a post-doctoral fellowship position at the "Polytechnic Institute of Advanced Sciences", Autonomous Aerial Systems Laboratory, France.

His research interests include modeling and control of convertible drones with interactive applications, time-delay systems and multi-agent control systems in the field of aerial robotics.

E-mail: jonatan.alvarez@ipsa.fr (Corresponding author)
ORCID iD: 0000-0003-1038-6800

N. Marchand received the M. Sc. and Ph. D. degrees in automatic control from Grenoble Institute of Technology, France in 1995 and 1999, repectively. He was temporary teaching and researcher (ATER) at the Technological University Institute of Villeurbanne, France. From 2000 to 2002, he was an assistant professor at Paris-Sud University and Signals and Systems Laboratory, France. In 2013, he obtained the habilitation to direct research (HDR) from University of Grenoble, France. Since 2013, he is the National Center for Scientific Research (CNRS) senior researcher. Currently, he is deputy director of GIPSA-Lab laboratory, France. His work is focused on the control of systems on chips and cloud systems and more recently privacy.

His research interests include theoretical and applicative topics: event-based control, asynchronous control of linear and non linear systems, control and stabilization of flying robots using bio inspired strategies and control theory for computer sciences.

E-mail: Nicolas.Marchand@gipsa-lab.fr

J. F. Guerrero-Castellanos received the B. Sc. degree in electronic science from Autonomous University of Puebla (BUAP), Mexico in 2002, and the M. Sc. and Ph. D. degrees in automatic control from Grenoble Institute of Technology and Joseph Fourier University, France, in 2004 and 2008, respectively. Between January and June 2008, he was a postdoctoral researcher at GIPSA-Lab Laboratory, France. After spending one year at the University Polytechnic of Puebla, Mexico as an assistant professor, he joined in 2009 Faculty of Electronics at BUAP, Mexico, as a full professor, where he established and directs the Control and Cyber-Physical Systems Laboratory. In 2016, he was a visiting research professor at the Laboratory of Image, Signal and Intelligent System (LISSI) – Paris-Est Creteil University (UPEC), France. Between August 2013 and December 2017, he was the head of Renewable Energy Engineering at BUAP, Mexico. He is a member of Mexican Academy of Science (AMC), Mexican Association on Automatic Control (AMCA), a member of IEEE and the National System of Researchers (Researcher Level I), Mexico.

His research interests include guidance and control of autonomous systems, wearable robots, microelectronics systems and control of renewable energy systems.

E-mail: fermi.guerrero@correo.buap.mx

J. J. Tellez-Guzman received the M. Sc. degree in electronics from Autonomous University of Puebla, Mexico in 2012. Currently, he is a Ph. D. degree candidate in automatic control at GIPSA-Lab, University of Grenoble (UGA), France.

His research interests include modeling and control of aerial vehicles and vision-based control in the field of aerial robotics.

E-mail: jose-juan.tellez-guzman@gipsa-lab.grenoble-inp.fr

J. Escareno received the Ph. D. degree in automatic control from HEUDIASYC Laboratory, University of Technology of Compiegne (UTC), France in 2008. He has held a post-doctoral fellowship position at International Joint Unit of CNRS, 3175 LAFMIA hosted by CINVESTAV, from 2008 to 2010. He was a CNRS project researcher at University of Technology of Compiegne, France from 2010 to 2012. In March 2012, he was a visiting researcher at the French Nuclear Energy Commission (CEA), France. From July 2012 to October 2013, he was post-doctoral research associate at the Department of "Control and Micro-Mechatronics Systems" (AS2M) at FEMTO-ST (Franche-Comté Electronics Mechanics Thermal et Optical) UMR CNRS 6174, France. Currently, he holds an associate professor

position at the "Polytechnic Institut of Advanced Sciences", France.

His research interests include design, modeling and control of convertible and interactive drones in the field of aerial robotics. Likewise within the field of microrobotics, he is interested on embedded perception and control of piezoelectric actuators for micro-positioning applications.

E-mail: juan-antonio.escareno@ipsa.fr

M. Rakotondrabe received the HDR in control systems from Bourgogne Franche-Comte University, France in 2014. He is an associate professor at Bourgogne Franche-Comte University since 2007 with research affiliation at Automatic Control and Micromechatronic Systems Department of FEMTO02-ST Institute. He was the leader of the CODE Group ("Control and Design" Group) at FEMTO-02ST from 2015 to 2017. Since 2017, he founded the MACS Group (Methodologies for the Automatic Control and for the Design of Mechatronic Systems). He also founded and is the head of the international master on Control for Green Mechatronics (GREEM) of the Bourgogne Franche-Comte University, all in France. He is or was associate or guest editor in prestigious journals related to Automation and micro and nano Mechatronics: *IEEE/ASME Transactions on Mechatronics*, *IFAC Mechatronics*, *IEEE Robotics and Automation Letters*, *IEEE Transactions on Industrial Electronics*, *MDPI Actuators*. In 2016, he is recipient of the Big02-On-Small award delivered during the *IEEE MARSS International Conference on Manipulation, Automation and Robotics at Small Scales*. This award is to recognize a young professional (less than 40 years old) with excellent performance and international visibility in the topics of mechatronics and automation for manipulation at small scales.

His research interests include design, modeling, signal estimation and control techniques for piezoelectric actuators in general and for microsystems.

E-mail: mrakoton@femto-st.fr